Hindawi Publishing Corporation
Journal of Nanomaterials
Volume 2014, Article ID 264108, 8 pages
http://dx.doi.org/10.1155/2014/264108

Research Article

Effect of Core-Shell Ag@TiO_2 Volume Ratio on Characteristics of TiO_2-Based DSSCs

Ho Chang,[1,2] Chih-Hao Chen,[3,4] Mu-Jung Kao,[5] and Hsin-Han Hsiao[1]

[1] *Graduate Institute of Manufacturing Technology, National Taipei University of Technology, Taipei 10608, Taiwan*
[2] *Department of Mechanical Engineering, National Taipei University of Technology, Taipei 10608, Taiwan*
[3] *Department of Thoracic Surgery, Mackay Memorial Hospital, Taipei 10449, Taiwan*
[4] *Mackay Junior College of Medicine, Nursing, and Management, Taipei 11260, Taiwan*
[5] *Department of Vehicle Engineering, National Taipei University of Technology, Taipei 10608, Taiwan*

Correspondence should be addressed to Ho Chang; f10381@ntut.edu.tw and Chih-Hao Chen; musclenet2003@yahoo.com.tw

Received 8 May 2014; Accepted 16 June 2014; Published 1 July 2014

Academic Editor: Chin-Guo Kuo

This paper aims to develop photoanode material required by dye-sensitized solar cells. The material prepared is in the form of Ag@TiO_2 core-shell-type nanocomposites. This material is used to replace the titanium oxide powder commonly used in general DSSCs. The prepared Ag@TiO_2 core-shell-type nanocomposites are mixed with Degussa P25 TiO_2 in different proportions. Triton X-100 is added and polyethylene glycol (PEG) at 20 wt% is used as a polymer additive. This study tests the particle size and material properties of Ag@TiO_2 core-shell-type nanocomposites and measures the photoelectric conversion efficiency and IPCE of DSSCs. Experimental results show that the DSSC prepared by Ag@TiO_2 core-shell-type nanocomposites can achieve a photoelectric conversion efficiency of 3.67%. When Ag@TiO_2 core-shell-type nanocomposites are mixed with P25 nanoparticles in specific proportions, and when the thickness of the photoelectrode thin film is 28 μm, the photoelectric conversion efficiency can reach 6.06%, with a fill factor of 0.52, open-circuit voltage of 0.64V, and short-circuit density of 18.22 $mAcm^{-2}$. Compared to the DSSC prepared by P25 TiO_2 only, the photoelectric conversion efficiency can be raised by 38% under the proposed approach.

1. Introduction

With the development of solar cells from single crystal, polycrystal, and amorphous silicon, to today's popular copper indium gallium selenide (CIGS), polymer solar cells and dye-sensitized solar cells (DSSC) have attracted extensive attention from academia and industry. Dye-sensitized solar cells (DSSCs) have attracted great interest as one of the most potential photovoltaic devices owing to their low cost and easy fabrication [1–3]. However, due to their disadvantages of low photoelectric conversion efficiency and short-period stability, DSSCs still have not been popularized [4].

In 1991 Grätzel of the Swiss Federal Institute of Technology in Lausanne used TiO_2 powder to prepare semiconductor thin film as a photoelectrode. After the photoelectrode was mixed with Ru-complex dye sensitizer and Redox electrolyte and then illuminated under sunlight, its photoelectric conversion efficiency could reach 7% [5, 6]. This kind of cell is called a dye-sensitized solar cell (DSSC). Due to its cheap cost compared to other kinds of solar cells, DSSCs have gradually attracted more and more attention. In recent years, the efficiency of DSSCs even has been increased to 11% [7]. Murray et al. developed core-shell-type semiconductor nanocomposites [8]. Their manufacturing process employed trioctylphosphine (TOP) taken as surfactant and trioctylphosphine oxide (TOPO) as the solvent to produce a synthesized product made in a high-temperature environment. Revaprasadu et al. used single-molecule precursors [$Cd(Se_2CNMe(Hex))_2$] and [$Cd(S_2CNMe(Hex))_2$] to carry out continuous thermal cracking and finally prepared CdSe@CdS core-shell-type semiconductor nanocomposites [9]. Furthermore, preparation of core-shell-type semiconductor nanocomposites by a water-in-oil method has also been achieved in recent years. Related studies have subsequently made nanocomposite particles of Au@Pb, Au@Sn, Au@Tl, Ag@Pb, Ag@Cd, and Ag@In; the optical properties of these particles have revealed

blue shift phenomenon, where shell layer atoms provide electrons to core layer particles [10].

Core-shell double-metal nanoparticles are mainly prepared and acquired by chemical reduction of the liquid phase. Rivas et al. firstly used citric acid to prepare Au nanoparticles and then used ascorbic acid to perform reduction of the Ag particles of sedimentary shell [11]. Mulvaney et al. used γ-ray to produce free radicals in solution and further carried out reduction of the metallic salt of shell [12]. As for nanocomposites composed of oxide, the main research targets of oxide have been SiO_2, ZrO_2, and SnO_2 nanomaterials with optical transparency, TiO_2 nanomaterial with photocatalytic and photoelectric semiconductor effects, and magnetic Fe_2O_3 and Fe_3O_4 nanomaterials [13–16]. In 2011, Qi et al. of the Massachusetts Institute of Technology used the surface plasmon effect of Ag to increase the sunlight absorption of dye and as a result improved the efficiency from 3.1% to 4.4% [17]. Ag@TiO_2 core-shell-type nanocomposites have excellent visible light transparency [18]. Complete TiO_2 coating can effectively protect the Ag metal inside, preventing it from being corroded and affected by the external environment. Thus, this type of nanocomposite possesses the properties of both Ag nanometal and TiO_2 photoelectric material and effectively extends the life of material. Ag nanoparticles have the property of surface plasmon resonance, making it possible to absorb visible light and to excite the electron and hole. Moreover, TiO_2 has the unique property of ultraviolet absorption. Therefore, applying Ag@TiO_2 nanocomposites to DSSCs can effectively extend photoelectric reaction from the ultraviolet zone to the visible light zone. Furthermore, Ag@TiO_2 nanocomposites have excellent visible light transparency. Through the piling up of tiny nanoparticles, a porous structure is formed. This helps to increase the photoanode surface area. Below, this paper further analyzes the particle size and material.

This study mixes Ag@TiO_2 core-shell-type nanocomposite nanopowder with TiO_2 nanoparticles (Degussa P25 TiO_2) in suitable proportions (the mixing proportions of Ag@TiO_2 core-shell-type nanocomposite nanopowder and Degussa P25 TiO_2 nanoparticles are 10 : 0, 7 : 3, 5 : 5, 3 : 7, and 0 : 10). The mixed powder is made into a paste for coating on FTO conductive glass to carry out thermal treatment at 450°C. After simple packaging, DSSC components are made. This study investigates the surface structure and photoelectric conversion efficiency of core-shell-type photoanode structure.

2. Experimental Details

Using the chemical reduction method, the study prepares nano-Ag for an experiment. After metallic precursor salt is dissolved in the solvent, reduction of metallic ions is performed by a reducing agent, achieving pure Ag metallic nanoparticles [19]. After that, TiO_2 nanomaterial is coated on the surface of the metallic nanoparticles. Alcohol titanyl precursor salt is dispersed in ethanol solution. The solution is added to the prepared nano-Ag solution to carry out hydrolysis. Polycondensation is carried out through low-temperature heating and drying, and Ag@TiO_2 core-shell-type nanocomposites are synthesized [20].

The solution is preblended for direct use through the following steps.

(a) Weigh 0.1822 g of cetyl trimethylammonium bromide (CTAB) powder and dissolve it in 500 mL of pure water so as to prepare 1 mM of CTAB aqueous solution.

(b) Weigh 0.1699 g of silver nitrate ($AgNO_3$) powder and dissolve it in 20 mL of pure water so as to prepare 50 mM of $AgNO_3$ aqueous solution.

(c) Absorb 48.6 mL of hydrazine (N_2H_5OH) solution and dissolve it in 10 mL of pure water so as to prepare 100 mM of N_2H_5OH aqueous solution.

Absorb 1 mM of CTAB and 20 mL of aqueous solution in a sample bottle and stir the bottom using a magnet. In a water bath environment at 30°C, absorb 100 mM of N_2H_5OH aqueous solution. Add 0.5 mL to the CTAB solution and stir it well using a magnet until it is mixed evenly. In a water bath environment at 30°C, absorb 50 mM of $AgNO_3$ aqueous solution. Add 0.5 mL slowly to the CTAB and N_2H_5OH aqueous solutions made in the above steps and stir them using a magnet for 10 minutes to elicit a reaction. An evenly dispersed yellowish transparent pure Ag nanoparticle solution is obtained. This dispersion solution can be provided for subsequent synthesis of Ag@TiO_2. Advanced preparation of the solution for convenient and direct use is carried out as follows: absorb 7.45 μL of titanium isopropoxide (TTIP) solution and evenly disperse 25 mL of ethanol so as to prepare 1 mM of TTIP ethanol solution.

The prepared pure Ag nanoparticle solution is poured into a 100 mL serum bottle. Stir the bottom continuously using a magnet. Slowly pour 25 mL of pure Ag nanoparticle solution several times into the 1 mM of prepared TTIP methanol solution and stir the bottom intensely using a magnet. Continue stirring intensely for 10 minutes. Use a test tube oscillator to carry out a continuous oscillating reaction for 1 hour. Then TiO_2 can completely coat the surface of pure Ag nanoparticles and achieve a Ag@TiO_2 core-shell-type nanocomposite solution. Centrifugal separation is conducted on the acquired Ag@TiO_2 core-shell-type nanocomposites, and they are washed by ethanol and pure water several times. After they are dried in oven at 60°C, Ag@TiO_2 core-shell-type nanocomposite powder is obtained for further analysis. Comparing the photoelectric conversion efficiencies for mixtures of Ag@TiO_2 core-shell-type nanocomposite nanopowder and Degussa P25 TiO_2 in different proportions, this study selects 5 representative mixing proportions for application to photoanodes thin film in DSSCs. The five representative mixing proportions of Ag@TiO_2 core-shell-type nanocomposite nanopowder and Degussa P25 TiO_2 nanoparticles are 10 : 0, 7 : 3, 5 : 5, 3 : 7, and 0 : 10.

The conductive glass material selected for the photoanode and counter electrode in this study is fluorine-doped tin oxide (FTO). First of all, the conductive glass is cut into the size 2.5 cm $*$ 2 m and then placed in acetone. After being

oscillated in an ultrasonic oscillator for 10 minutes, the conductive glass is washed by deionized water and then placed in anhydrous methanol to be oscillated in an ultrasonic oscillator for another 10 minutes. After the conductive glass is washed by deionized water and dried in an oven, adhesive tape is stuck on the conductive side of the conductive glass. An area of 1 cm $*$ 1 cm is left in the middle to be coated by the well-blended Ag@TiO_2 core-shell-type nanocomposite paste by a spin coater for 10 seconds, with spinning speeds set at 500 rpm, 800 rpm, 1000 rpm, and 1200 rpm to produce thin films of different thicknesses. The advantage of using spin coating method was that the acquired thin film could have even thickness. The coated conductive glass is firstly placed in the oven at 50°C to be dried for 10 minutes. After that, the adhesive tape is removed from the conductive glass, which is then placed in a sintering furnace. The sintering process is to let temperature rise (at 10°C/min) to 70°C, which is kept unchanged for 15 minutes. After that, the temperature is increased (at 10°C/min) to 400°C and then kept unchanged for 30 minutes, completely changing the TiO_2 into a pure anatase phase. Anatase TiO_2 has better photoelectric properties. After heating is completed, it is placed in the oven for natural cooling to room temperature. Then the preparation of photoanode thin film is complete.

For the preparation of the counterelectrode thin film, a platinum (Pt) thin film with a thickness of around 20 nm is sputtered on the surface of FTO conductive glass, with sputtering parameters set at vacuum degree of 6 Pa, electric current value of 30 mA, and sputtering time of 120 seconds. After completion of sputtering, Teflon adhesive tape is stuck on the thin film surface, with an area of 0.5 cm $*$ 0.5 cm left illuminated.

Next, the photoanode is soaked in N719 dye for 24 hours, without light illumination from the outside and under a suitable temperature, and the dye residue on the surface is washed away by acetonitrile. The photoanode and counter electrode are superimposed as a sandwich assembly. An electrolyte is injected into the gap between photoelectrode and counter electrode, but air bubbles should not be produced. Finally, the two sides are fixed by foldback clips, and a segment of copper paste is stuck on the conductive side of counter electrode in order to increase and strengthen its conductivity for subsequent testing. Then, the simple packaging of the DSSC is completed. After completion of assembly, the light of a xenon (Xe) lamp at 150 W is used to simulate sunlight (AM 1.5) and combined with a Keithley 2400 to assemble as an *I-V* curve analyzer. Before testing, the distance between the light source and sample should be adjusted, and the light density is set at 100 mW/cm^2. With the measurement results, an *I-V* curve can be obtained. Based on the *I-V* curve, this study further acquires V_{oc} (V), J_{sc} (mA/cm^2), FF, and η%.

3. Results and Discussion

Through SEM analysis, the appearance, particle size, and hole size of Ag@TiO_2 core-shell-type nanocomposites can be directly observed. Figure 1(a) shows the surface structure of Ag@TiO_2 core-shell-type nanocomposite powder. The figure

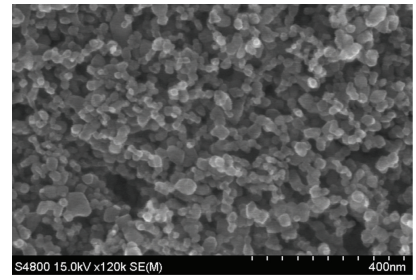

(a)

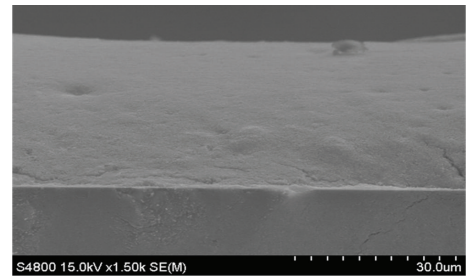

(b)

Figure 1: (a) FE-SEM image and (b) cross-section of the prepared Ag@TiO_2 core-shell thin film formed by spin coating.

shows that, through the piling up of many tiny nanoparticles, Ag@TiO_2 photoanode forms a porous structure. As observed in the figure, Ag@TiO_2 holes are looser. The porous structure possesses not only great surface area, but also good absorption of N719 dye. Meanwhile, it aids in the penetration of the electrolyte. This is believed to effectively enhance the efficiency of the photoelectric chemical reaction. Figure 1(b) shows a cross-section of a lateral view of the SEM image. It can be observed that the thickness of Ag@TiO_2 photoanode thin film is 28 μm. The holes of Ag@TiO_2 photoanode thin film are looser. Nevertheless, the loose structure of the holes is helpful for penetration of the electrolyte. This is expected to enhance the results of photoelectric chemical reaction more effectively. Moreover, as observed from the cross-section of the SEM image, a FTO conductive glass layer of around 0.9 μm is found on the lower layer. After thermal treatment, the binding force between the thin film and the glass is increased, proving that a path is formed after the Ag@TiO_2 photoanode thin film contacts the conductive glass layer and also indicating that this working electrode can really carry out a photoelectric chemical reaction.

The appearance of the Ag@TiO_2 core-shell-type nanocomposite powder synthesized in this study reveals even spherical particles, and very excellent dispersion, without agglomeration. Figures 2(a), 2(b), and 2(c) are general TEM photographs and HR-TEM photographs. After careful observation of each particle, it is found that the original particles with darker color inside are Ag particles, which are externally coated by light grayish TiO_2 shells, directly showing that this study successfully synthesizes core-shell-type nanocomposite structure. As observed from the analysis results of Figures 2(a) and 2(c), the particle size of the Ag@TiO_2 core-shell-type nanocomposites is

Table 1: Composition analysis of the Ag core by EDS.

Element	Weight%	Atomic%
O	9.93	41.48
Ti	3.51	4.9
Ag	86.56	53.63
Total	100.00	100.00

Table 2: Composition analysis of the TiO_2 shell by EDS.

Element	Weight%	Atomic%
O	67.37	86.29
Ti	31.58	13.51
Ag	1.05	0.2
Total	100.00	100.00

10.5 nm. Based on particle size distribution of Ag@TiO_2, the core diameter of Ag is estimated to be around 9.5 nm, and the diameter of the shell is around 1 nm. The TiO_2 shell does not show any noticeable change of core size. In Figure 2(c), the lattice structure of the Ag core can be clearly seen, and the structure of the TiO_2 shell appears to be in the noncrystalline phase. The results shown in the TEM and HR-TEM photographs can prove that the synthesized Ag@TiO_2 has complete nanocomposite structure and is evenly coated.

Using the EDS attached to the TEM, this study focuses on Figure 2(c) to carry out composition analysis of the Ag core and TiO_2 shell by acquiring the composition structure of this single area. As seen in Table 1, when composition analysis of the core is carried out, the elements of Ag appear to have a very strong plasmon absorption band. When focusing on the part of shell, the plasmon absorption band of Ag cannot be observed (Table 2), proving that Ag@TiO_2 has a core-shell-type nanocomposite structure which really takes Ag as its core and TiO_2 as its shell.

The HR EDS mapping function attached to EDS can focus on a single Ag@TiO_2 core-shell particle to analyze the composition of its elements. Focusing on Figure 3, when the mapping function is performed on a single core-shell particle, Ag atoms are obviously found to be agglomerated in the core, which is evenly coated by O and Ti atoms. This clearly proves that Ag atoms are completely coated by TiO_2, and the outer shell is evenly dispersed. This also proves that Ag@TiO_2 has a core-shell-type nanocomposite structure, which really takes Ag as the core and TiO_2 as the shell.

This study analyzes and tests the XRD crystalline phase structure of Ag@TiO_2 core-shell particles using an X-ray powder diffractometer. After comparison with the database published by Joint Committee on Powder Diffraction Standard (JCPDS), the results are shown in Figure 4. From the XRD analytic results before calcinations of Ag@TiO_2 core-shell-type nanocomposites shown in Figure 4(a), Ag@TiO_2 appears to have obvious face-centered cubic (FCC) pure Ag metallic structure. The main plasmon absorption bands 2θ = 38°, 44°, 64°, and 77° are consistent with FCC pure Ag metals (111), (200), (220), and (311), respectively, indicating

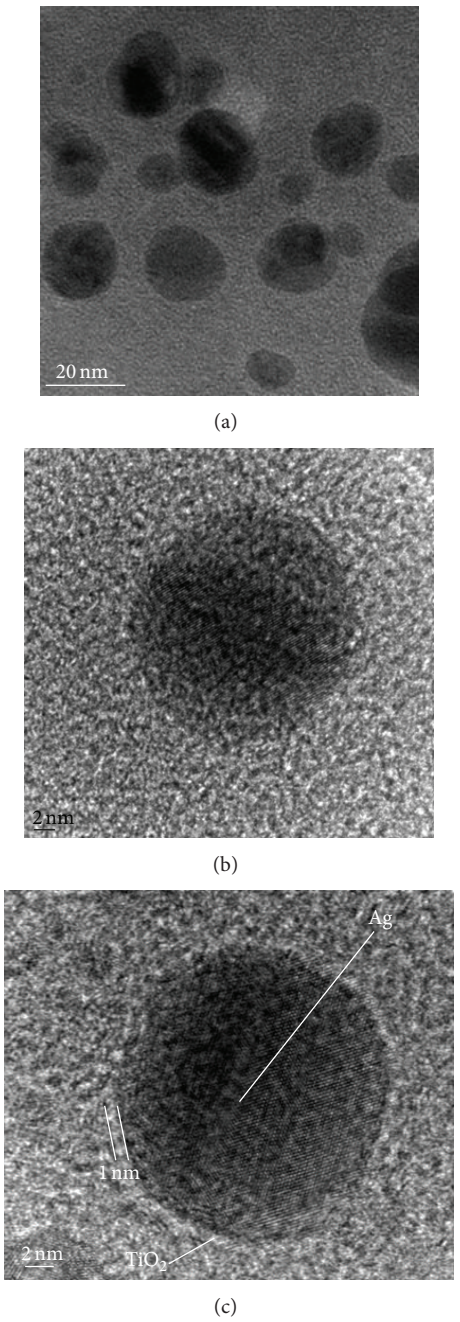

Figure 2: (a) TEM image of Ag@TiO_2 core-shell. (b) HR-TEM image of Ag nanoparticle. (c) HR-TEM of Ag@TiO_2 core-shell.

that even though TiO_2 coating is applied the Ag core still has not been oxidized. Nevertheless, XRD analysis before sintering of Ag@TiO_2 shows no plasmon absorption band belonging to TiO_2, indicating that the shell with TiO_2 coating has a noncrystalline phase structure. This may be because when TiO_2 is coated on the outer layer of Ag, as affected by the core of metal and restricted by thinner thickness, the crystalline phase growth of TiO_2 shell is suppressed, thus leading to this noncrystalline phase structure. Moreover, it is noteworthy that, in the XRD analysis after calcination

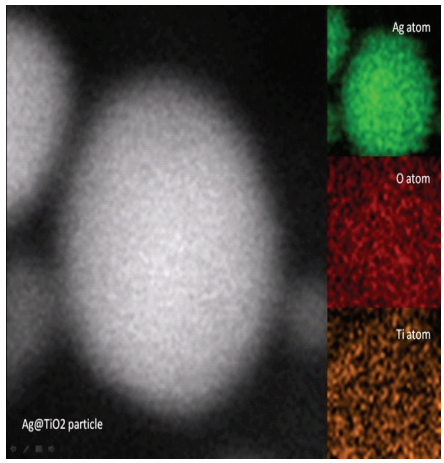

Figure 3: EDS mapping of Ag@TiO_2 core-shell. The images on the right-hand side from the top to the bottom show the atomic distribution of Ag, O, and Ti, respectively.

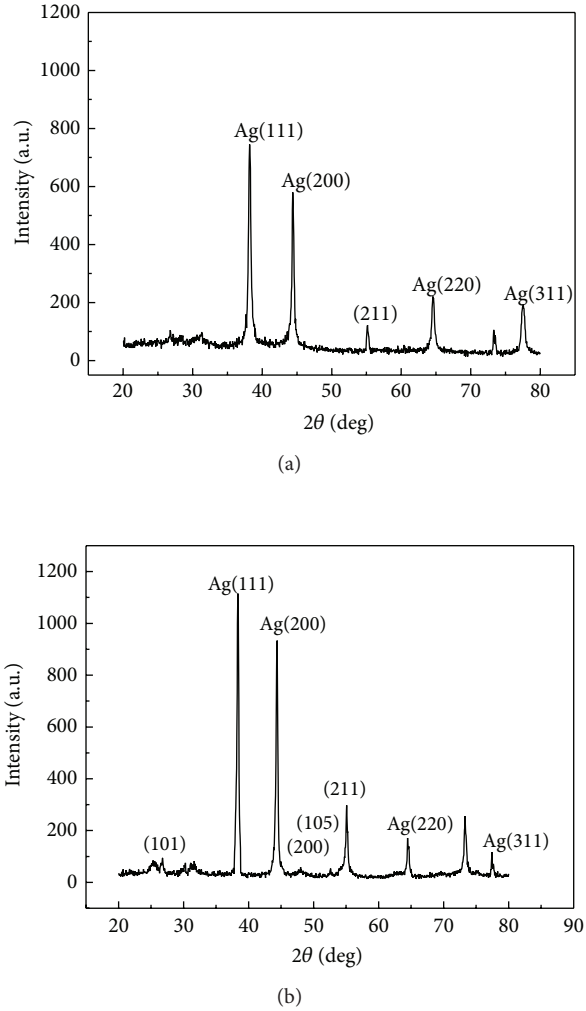

Figure 4: XRD analysis of DSSCs with Ag@TiO_2 core-shell structure (a) before and (b) after calcination.

of Ag@TiO_2 core-shell-type nanocomposites at 400°C for 1 hour, the Ag is also not oxidized (Figure 4(b)). This indicates that even when calcination is performed under high temperature 400°C for 1 hour the Ag core still maintains its pure metallic properties, without any sign of being oxidized. This also reveals the protective effect of TiO_2 for the outer layer. Nevertheless, besides the plasmon absorption band of Ag, some weak signals can still be found, such as where the plasmon absorption bands 2θ = 25.3°, 30.5°, and 50.5° just meet the (101) crystalline surface of pure anatase TiO_2 and the signals of the FTO conductive layer. This clearly shows that, under calcinations at high temperature 400°C for 1 hour, the TiO_2 shell can transform from a noncrystalline phase into a weak pure anatase structure. Its plasmon absorption bands are at positions 2θ = 25.3°, 48.1°, 53.9°, and 54.3°, which correspond to the crystalline sides (101), (200), (105), and (211) of pure anatase, respectively.

Through UV-Vis spectroscopic analysis, we can examine the optical properties of Ag@TiO_2 core-shell-type nanocomposites acquired in this study, and the absorption properties under ultraviolet and visible light can be understood. This study verifies the visible light absorption effect of such core-shell-type nanocomposites and compares it with commercially used TiO_2 nanoparticles (Degussa P25 TiO_2) for analysis. We use anhydrous ethanol as the substrate, with the addition of commercially used TiO_2 nanoparticles (Degussa P25 TiO_2) and Ag@TiO_2 core-shell-type nanocomposites to carry out oscillation by ultrasonic oscillator for 15 minutes, making them evenly dispersed in anhydrous ethanol. A quartz tube is placed in the machine. Spectroscopy is used to measure the light absorption strength of P25 TiO_2 and Ag@TiO_2 core-shell-type nanocomposites. Figure 5 shows the UV-Vis absorption spectrum analysis of Ag, Ag@TiO_2, and Degussa P25 TiO_2. Since the Ag nanoparticle has the property of surface plasmon resonance, it has very strong ability to absorb visible light. The main absorption peak is around the wavelength of 410 nm. Degussa P25 TiO_2 and Ag@TiO_2 core-shell-type nanocomposites are in the ultraviolet zone at 250~380 nm, and both have good absorption ability. This is because of TiO_2's unique ultraviolet absorption property. Since the Ag nanoparticle has the property of surface plasmon resonance, it has very strong ability to absorb visible light. After coating the outer layer TiO_2, the absorption peak of Ag@TiO_2 redshifts from 360 nm to 450 nm. This is mainly because the outer TiO_2 shell has a high refraction rate and completely coats the Ag core, leading to an obvious redshift of the absorption peak for 90 nm. The absorption peak extends from the ultraviolet zone to the visible light zone. Such an obvious redshift really proves that the absorption wavelength range of photoelectric conversion increases.

Ag@TiO_2 core-shell-type nanocomposite nanopowder is mixed with TiO_2 nanoparticles (Degussa P25) in suitable proportions. The mixing proportions of Ag@TiO_2 core-shell-type nanocomposite nanopowder and Degussa P25 nanoparticles are 10 : 0, 7 : 3, 5 : 5, 3 : 7, and 0 : 10. The mixed powder is made into paste for coating on FTO conductive glass so as to carry out thermal treatment at 450°C. After simple packaging, DSSC components are made, and the performance of DSSC components is analyzed.

Table 3: The photovoltaic performance of composite photoelectrode materials in different proportions and with the same photoanode thickness.

Sample $Ag@TiO_2$: P25 TiO_2	Thickness (μm)	V_{oc} (V)	J_{sc} (mA/cm^2)	FF	η (%)
100 : 0	26	0.651	11.3	0.492	3.64
70 : 30	26	0.64	13.18	0.505	4.27
50 : 50	26	0.66	15.65	0.448	4.62
30 : 70	26	0.64	17.01	0.51	5.55
0 : 100	26	0.64	16.62	0.413	4.4

Table 4: The photovoltaic performance of photoanodes with different thicknesses and the same proportion of composite photoelectrode materials.

Sample $Ag@TiO_2$: P25 TiO_2	Thickness (μm)	V_{oc} (V)	J_{sc} (mA/cm^2)	FF	η (%)
30 : 70	24	0.65	13.628	0.584	5.18
30 : 70	26	0.64	17.01	0.51	5.55
30 : 70	28	0.64	18.22	0.52	6.06
30 : 70	30	0.66	16.03	0.54	5.7

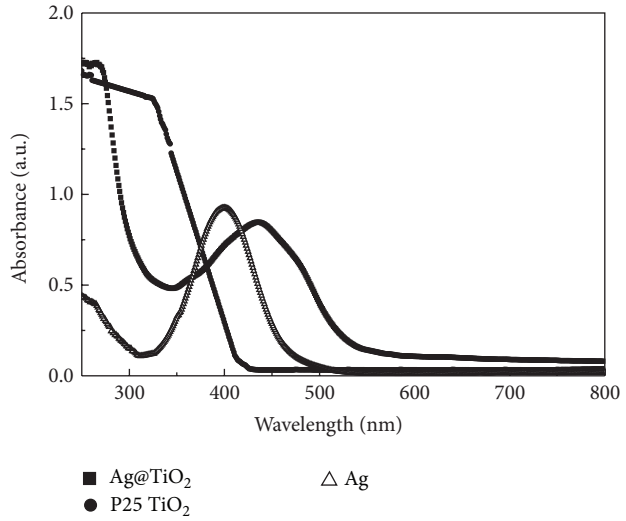

Figure 5: Absorption spectrum of P25 TiO_2, Ag, and $Ag@TiO_2$ core-shell.

As shown in the test results in Figure 6 and Table 3, when the mixing proportion of $Ag@TiO_2$ core-shell-type nanocomposite nanopowder and Degussa P25 TiO_2 nanoparticles is 3 : 7, an optimal photoelectric conversion efficiency of 5.5% is achieved. Since the transmission of electrons does not get faster after Degussa P25 TiO_2 nanoparticles are added to $Ag@TiO_2$ core-shell-type nanocomposite nanopowder, light scattering ability can be increased. Furthermore, since the Ag core has the property of surface plasmon resonance, it can effectively absorb visible light. Its role is similar to the dye in a DSSC, helping the $Ag@TiO_2$ photoelectrode to achieve very effective absorption in the visible light zone. As for the other mixing proportions of $Ag@TiO_2$ core-shell-type nanocomposite nanopowder and Degussa P25 TiO_2 nanoparticles at 10 : 0, 7 : 3, 5 : 5, and 0 : 10, according to the tests, the photoelectric conversion efficiencies of their photoelectrode thin films are 3.6%, 4.2%, 4.6%, and 4.4%, respectively. Amongst them, for the components of $Ag@TiO_2$ core-shell-type nanocomposite nanopowder in the proportion of 100 : 0, it is estimated that the proportion of anatase TiO_2 is not enough. Therefore, the photoelectric conversion efficiency result is not as good as expected. The product information of Degussa P25 TiO_2 shows that anatase occupies 3/4 of the entire product. Thus, after Degussa P25 TiO_2 powder is added at a fixed percentage of 30%, the synthesized $Ag@TiO_2$ core-shell-type nanocomposite nanopowder significantly enhances the photoelectric conversion efficiency. For Degussa P25 TiO_2 nanoparticles with the proportion of 0 : 100, the thickness of 26 μm is estimated to be rather high. Thus, the transmission distance of the electrons excited by dye on the TiO_2 of conductive glass surface is lengthened. Under this process, the electrons can recombine with electrolytes more easily. Therefore, the photoanode thin film is thicker. Although more electrons can be produced, the electrons cannot be completely and effectively guided to FTO glass, resulting in an efficiency of 4.4%.

When the mixing proportion of $Ag@TiO_2$ core-shell-type nanocomposite nanopowder and Degussa P25 TiO_2 nanoparticles is 30 : 70, different thin film thicknesses of components are tested in order to find the optimal thin film thicknesses. As proved by experiments, under the condition of spin coating speeds at 500 rpm, 800 rpm, 1000 rpm, and 1200 rpm, the prepared thin film thicknesses were around 24, 26, 28, and 30 μm, respectively. This study also explores the mutual effects of thin film thickness and photoelectric conversion efficiency. Experimental results show that when the thickness of the photoelectrode film is 28 μm, DSSC components achieve an optimal photoelectric conversion efficiency of 6.06%. When the film thickness is 26 μm,

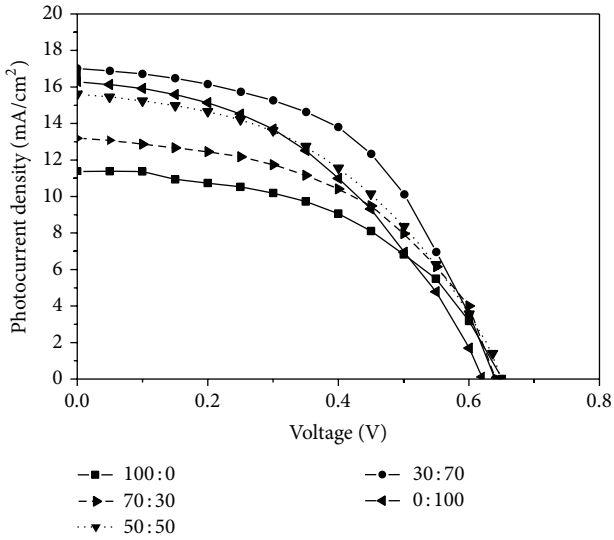

Figure 6: Dependence of photocurrent density J_{sc} and conversion efficiency of DSSCs comprised of composite photoelectrode materials in different proportions.

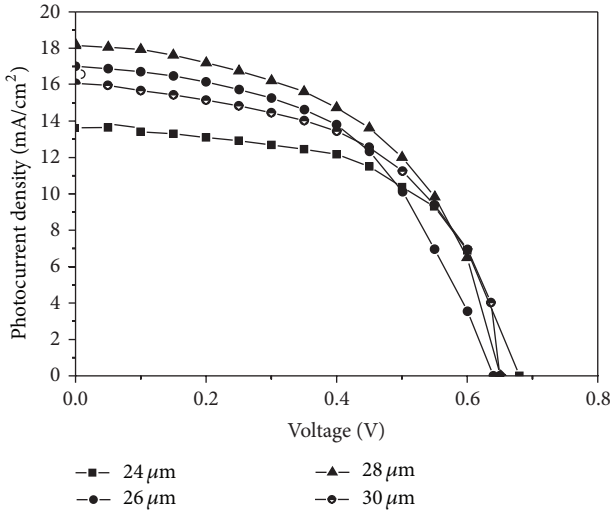

Figure 7: Photocurrent density J_{sc} and conversion efficiency of DSSCs comprised of photoanodes in different thicknesses.

the photoelectric conversion efficiency is 5.55%, and the optimal photocurrent density of 18.22 mA/cm^2 is achieved. When the film thickness of the components is 24 μm, the photoelectric conversion efficiency is reduced to 5.18% and the photocurrent density is 13.628 mA/cm^2. As seen from the test results, photoelectrode thickness and photoelectric conversion efficiency are closely related, but there is not an absolute linear relationship. Related test results are shown in Figure 7 and Table 4.

With the increase of film thickness, photoelectric conversion efficiency and photocurrent density both fall after reaching their maximum values. This could be attributed to the following reasons. Firstly, with the increase of thin film thickness, tiny air bubbles can easily be produced in coating material. In this case, when the photoanode is sintered at 400°C, collapse and cracking occurs. Secondly, with the increase of thin film thickness, the translucence of the photoanode declines. When photoelectric conversion efficiency is tested, incident light cannot penetrate the bottom layer of the thin film effectively. Dye molecules thus jump into an excited state and the production of photoelectrons is restricted. As a result, higher photoelectric conversion efficiency cannot be obtained.

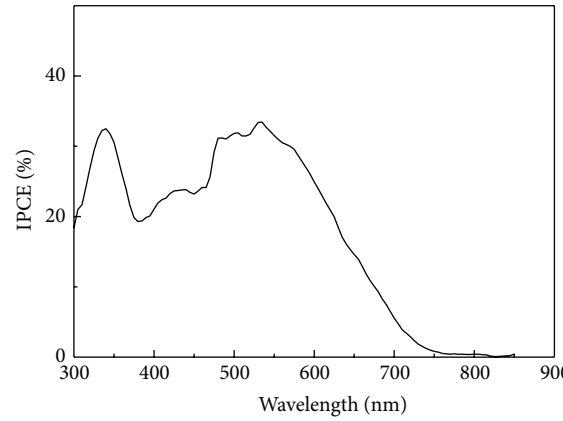

Figure 8: IPCE curves of the prepared DSSCs.

Figure 8 shows the test results of the incident photon-electron conversion efficiency (IPCE) of Ag@TiO_2 core-shell-type nanocomposite powder. The absorption band of N719 dye is 500~600 nm. The figure also shows clearly that the peak value is at wavelength of 550 nm, indicating that after absorption of incident light at such a wavelength range the excited electrons in N719 dye have completed transmission and produced electric energy. According to the previously mentioned equation, the photocurrent value (J_{sc}) is the integration of IPCE value to wavelength (λ). When the numerical value is higher, the converted numerical photocurrent value increases. As seen in Figure 8, the component has a maximum IPCE value of around 35% at the wavelength of 550 nm.

4. Conclusion

This study explores the preparation of TiO_2 nanoparticles and core-shell-type nanocomposites of Ag metal and provides related analysis. Comparing the photoelectric conversion efficiencies for mixtures of Ag@TiO_2 core-shell-type nanocomposite nanopowder and Degussa P25 TiO_2 in different proportions, this study finds the optimal film thickness for application to photoanodes in DSSCs. Experimental results show that the photoelectrode thin film prepared at the mixing proportion of 3 : 7 with Ag@TiO_2 core-shell-type nanocomposite nanopowder and Degussa P25 TiO_2 nanoparticles achieves a thin film thickness of around 28 μm, fill factor of 0.52, open-circuit voltage of 0.64 V, and short-circuit density of 18.22 mAcm^{-2}. Compared to the DSSC prepared by Degussa P25 TiO_2, its photoelectric conversion efficiency can be enhanced by 38%.

Conflict of Interests

The authors declare that there is no conflict of interests regarding the publication of this paper.

Acknowledgment

This study was supported by the National Science Council of Taiwan, Taiwan, under Project Grant no. NSC 100-2221-E-027-012.

References

[1] L. Song, Q. Jianga, P. Dua, Y. Yang, J. Xiong, and C. Cui, "Novel structure of TiO_2-ZnO core shell rice grain for photoanode of dye-sensitized solar cells," *Journal of Power Sources*, vol. 261, pp. 1–6, 2014.

[2] B. Liu and E. S. Aydil, "Growth of oriented single-crystalline rutile TiO_2 nanorods on transparent conducting substrates for dye-sensitized solar cells," *Journal of the American Chemical Society*, vol. 131, no. 11, pp. 3985–3990, 2009.

[3] Y. Y. Zhang, J. Khamwannah, H. Kim, S. Y. Noh, H. Yang, and S. Jin, "Improved dye sensitized solar cell performance in larger cell size by using TiO2 nanotubes," *Nanotechnology*, vol. 24, no. 4, Article ID 045401, pp. 1–6, 2013.

[4] M. H. Abdullah and M. Rusop, "Improved performance of dye-sensitized solar cell with a specially tailored TiO_2 compact layer prepared by RF magnetron sputtering," *Journal of Alloys and Compounds*, vol. 600, no. 5, pp. 60–66, 2014.

[5] B. O'Regan and M. Grätzel, "Low-cost, high-efficiency solar cell based on dye-sensitized colloidal TiO_2 films," *Nature*, vol. 353, no. 6346, pp. 737–740, 1991.

[6] A. Hagfeldt and M. Graetzel, "Light-induced redox reactions in nanocrystalline systems," *Chemical Reviews*, vol. 95, no. 1, pp. 49–68, 1995.

[7] M. A. Green, K. Emery, Y. Hishikawa, and W. Warta, "Solar cell efficiency tables (Version 33)," *Progress in Photovoltaics: Research and Applications*, vol. 17, no. 1, pp. 85–94, 2009.

[8] C. B. Murray, D. J. Norris, and M. G. Bawendi, " Synthesis and characterization of nearly monodisperse CdE (E = sulfur, selenium, tellurium) semiconductor nanocrystallites," *Journal of the American Chemical Society*, vol. 115, no. 19, pp. 8706–8715, 1993.

[9] N. Revaprasadu, M. A. Malik, P. O'Brien, and G. Wakefield, "Deposition of zinc sulfide quantum dots from a single-source molecular precursor," *Journal of Materials Research*, vol. 14, no. 8, pp. 3237–3240, 1999.

[10] J. Zhu, Y. Wang, L. Huang, and Y. Lu, "Resonance light scattering characters of core-shell structure of Au-Ag nanoparticles," *Physics Letters A*, vol. 323, no. 5-6, pp. 455–459, 2004.

[11] L. Rivas, S. Sánchez-Cortes, J. V. García-Ramos, and S. Sánchez-Cortes, "Mixed silver/gold colloids: a study of their formation, morphology and surface-enhanced Raman activity," *Spectrochimica Acta A*, vol. 56, no. 12, pp. 2471–2477, 2000.

[12] P. Mulvaney, M. Giersig, and A. Henglein, "Electrochemistry of multilayer colloids: preparation and absorption spectrum of gold-coated silver particles," *The Journal of Physical Chemistry*, vol. 97, no. 27, pp. 7061–7064, 1993.

[13] A. Henglein and M. J. Giersig, "Radiolytic formation of colloidal tin and tin-gold particles in aqueous solution," *Journal of Physical Chemistry A*, vol. 98, no. 28, pp. 6931–6935, 1994.

[14] A. Henglein, P. Mulvaney, A. Holzwarth, T. E. Sosebee, and A. Fojtik, "Ber. Bunsenges," *The Journal of Physical Chemistry A*, vol. 96, pp. 754–759, 1992.

[15] A. Henglein, A. Holzwarth, and P. J. Mulvaney, "Fermi level equilibration between colloidal lead and silver particles in aqueous solution," *Journal of Physical Chemistry A*, vol. 96, no. 22, pp. 8700–8702, 1992.

[16] A. Henglein, P. Mulvaney, T. Linnert, and A. Holzwarth, "Surface chemistry of colloidal silver: reduction of adsorbed Cd2+ ions and accompanying optical effects," *Journal of Physical Chemistry*, vol. 96, no. 6, pp. 2411–2414, 1992.

[17] J. Qi, X. Dang, P. T. Hammond, and A. M. Belcher, "Highly efficient plasmon-enhanced dye-sensitized solar cells through metal@oxide core-shell nanostructure," *ACS Nano*, vol. 5, no. 9, pp. 7108–7116, 2011.

[18] B. Cheng, Y. Le, and J. Yu, "Preparation and enhanced photocatalytic activity of Ag@TiO_2 core-shell nanocomposite nanowires," *Journal of Hazardous Materials*, vol. 177, no. 1–3, pp. 971–977, 2010.

[19] H. Y. Chang and D. H. Chen, "In addition, composites such as Ag-ZnO, Ag-SiO_2, Ag-TiO_2," *Nanotechnology*, vol. 20, pp. 105704–105714, 2009.

[20] H. Y. Chang and D. H. Chen, "Structural characterization and self-assembly into superlattices of iron oxide-gold core-shell nanoparticles synthesized via a high-temperature organometallic route," *Journal of Nanoparticle Research*, vol. 10, pp. 233–241, 2008.